Int. J. Solids Structures Vol. 20, No. 5, pp. 439–454, 1984
Printed in Great Britain.

0020 7683/84 $3.00 + .00
Pergamon Press Ltd.

SINGULARITIES AT THE TIP OF A CRACK NORMAL TO THE INTERFACE OF AN ANISOTROPIC LAYERED COMPOSITE

T. C. T. TING and P. H. HOANG
Department of Civil Engineering, Mechanics and Metallurgy, University of Illinois at Chicago, P.O. Box 4348, Chicago, IL 60680, U.S.A.

(*Received* 8 *March* 1983; *in revised form* 18 *July* 1983)

Abstract—The order of stress singularities at the tip of a crack which is normal to and ends at an interface between two anisotropic elastic layers in a composite is studied. Assuming that the stress singularities have the form $r^{-\kappa}$, equations are derived for determining the order of singularities κ. If the materials on both sides of the interface are identical, $\kappa = \frac{1}{2}$ is a root of multiplicity three each of which can be identified with the singularity due to, respectively, a symmetric tensile stress applied at infinity, an antisymmetric plane shear stress and an antiplane shear stress applied at infinity. When the materials on both sides of the interface are not the same, there are in general three distinct roots for κ. Numerical examples for a typical high modulus graphite/epoxy and for a special T300/5208 graphite/epoxy show that κ has three positive roots all of which are close to $\frac{1}{2}$ for most combinations of ply-angles in the two materials.

1. INTRODUCTION

Lightweight composite materials have been used for many years in the aerospace industries. Some of the most needed design informations are the failure mechanism and the failure criteria. Determination of the failure mechanism and the failure criteria requires in general rigorous stress analysis at the singular point in the material. The lack of such an analysis is one of the impediments in understanding the failure mechanism and in determining the failure criteria. In the case of layered composite materials in which each layer is of orthotropic material, experimental observations indicate that the failure modes are in general either along the interface between the layers or transverse to the layers. For instance, consider the layered composite shown in Fig. 1 in which each layer is a fiber reinforced composite laminate. The fibers lie in the plane of the layers although the orientation θ of the fibers may vary from layer to layer. When the composite is subjected to an extensional strain in the x_3-direction, a delamination may occur along the free-edge MN. The stress singularities at the free-edge such as the point M were investigated in [1]. It was shown in [1] that, except for certain special combinations of the ply-angles on both sides of the interface, the stresses have the logarithmic singularity at the free-edge in addition to the $r^{-\kappa}$ $(\kappa > 0)$ singularity. Moreover, unlike the $r^{-\kappa}$ singularity whose existence depends on the stacking sequence of the layers and the complete boundary conditions, the existence of the logarithmic singularity at point M depends only on the ply-angles on both sides of the interface. Instead of the delamination, a transverse crack shown by the dashed line may occur in the layer. There are stress singularities along the transverse crack edge MQ which is on the interface between two layers and hence may initiate a delamination along the interface. The nature of the singularities at the crack edge such as point 0 is the main interest of this investigation.

For this purpose, we take point 0 as the origin of the rectangular coordinate system (x_1, x_2, x_3) in which the $x_2 = 0$ plane is the interface while the transverse crack lies on the $x_3 = 0$ plane, Fig. 1. In the (x_2, x_3) plane, Fig. 2, the x_3-axis is the interface between the two materials and a crack in material 1 is located along the negative x_2-axis. The deformation at and near the origin 0 is certainly three-dimensional, i.e. the displacements

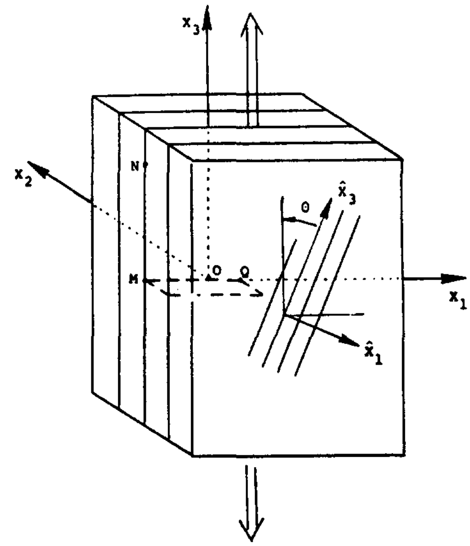

Fig. 1. Geometry of an angle-ply laminated composite.

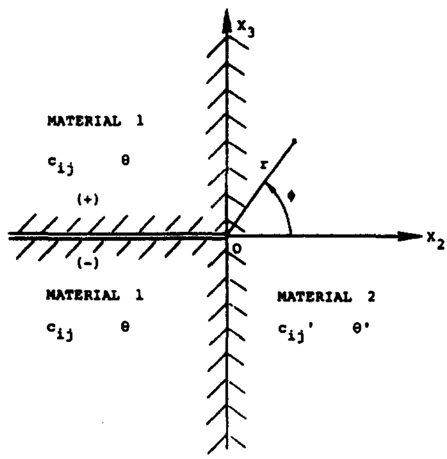

Fig. 2. A crack which is normal to and ends at the interface between two anisoptropic materials.

u_i are functions of x_2, x_3 as well as x_1. However, it was shown in [2] that, to the first order of approximation, the order of singularity at point 0 is affected by the dependence on x_1 only to the extent of the strain component ϵ_{11} at point 0. Since the problem is linear, we will first study the singularity at point 0 due to the displacement field in which u_i are functions of x_2 and x_3 only. We will then study the singularity at point 0 due to a uniform extension in the x_1-direction and see if additional singularities are present.

When the materials on both sides of the interface are isotropic, the singularity at the tip of a crack which is normal to and ends at the interface has been studied by many investigators (see [3–8], for example). In real composites, each layer is fiber reinforced laminated material and hence should be regarded as an anisotropic material. The problem of a crack terminating at the interface of two anisotropic materials does not seem to have been investigated, although the case of orthotropic materials was studied in [9, 10]. In Section 2 we present the basic formulations for anisotropic materials in two-dimensional deformation. Instead of using Lekhnitskii's approach [11] which breaks down in degenerate cases [12] and requires a special treatment for the degenerate cases, we employ the analysis which was originally due to Stroh [13] and further developed by others [14, 15] for studying surface waves in anisotropic elastic solids. In Section 3 we study the stress singularities at a crack tip in a homogeneous anisotropic elastic material, i.e. the material is not layered. The same problem was studied in [16, 17] for anisotropic elastic solids whose material property is symmetric with respect to the $x_1 = 0$ plane, and in [18, 19] for general anisotropic materials. By a different approach from that of [16–19], we show that $\kappa = 0.5$ is a triple root singularity for a crack tip in a homogeneous anisotropic medium. In Section 4 we formulate the equations for determining the order of singularities at the tip of a crack which is normal to and ends at an interface between two general anisotropic materials. We also show how one can determine the number of roots κ in a given region in the complex κ-plane. Numerical examples are presented in Section 5 in which both materials across the interface are of the same orthotropic materials although the orientations of the axes of symmetry are different. It is shown that there are three positive roots for κ and that all three have the values between 0.333 and 0.698. The fact that we have three positive κ and that they are near the value 0.5 is not surprising in view of the results obtained in Section 3 for the crack in a homogeneous anisotropic medium. Finally, in Section 6 we study the stress distribution near the tip of the crack which is normal to the interface subject to a uniform extensional strain in the x_1-direction. We show that a uniform stress solution exists and hence no additional stress singularity is present due to the uniform extension.

2. ANISOTROPIC MATERIAL IN TWO-DIMENSIONAL DEFORMATION

In the rectangular coordinate system (x_2, x_3), let the displacements u_i $(i = 1, 2, 3)$ and hence the strains ϵ_{ij} and the stresses σ_{ij} be functions of x_2 and x_3 only. The strain-displacement, stress–strain and equilibrium equations can be written as

$$\epsilon_{ij} = (\partial u_i/\partial x_j + \partial u_j/\partial x_i)/2 \tag{1}$$

$$\sigma_{ij} = c_{ijkp}\epsilon_{kp} \tag{2}$$

$$\partial\sigma_{i2}/\partial x_2 + \partial\sigma_{i3}/\partial x_3 = 0 \tag{3}$$

where repeated indices imply summation and

$$c_{ijkp} = c_{jikp} = c_{kpij} \tag{4}$$

are the elasticity constants. A general solution for eqns (1)–(3) can be obtained by letting

$$u_i = v_i f(Z) \tag{5}$$

$$Z = x_2 + px_3 \tag{6}$$

where p and v_i are constants to be determined and f is an arbitrary function of Z [13–15]. Substituting into eqns (1)–(3) we obtain

$$\sigma_{ij} = \tau_{ij}\,\mathrm{d}f/\mathrm{d}Z \tag{7}$$

$$D_{ik}v_k = 0 \tag{8}$$

where

$$\tau_{ij} = (c_{ijk2} + pc_{ijk3})v_k \tag{9}$$

$$D_{ik} = c_{i2k2} + p(c_{i2k3} + c_{i3k2}) + p^2 c_{i3k3}. \tag{10}$$

For a non-trivial solution of v_i, it follows from eqn (8) that the determinant of D_{ik} must vanish. That is,

$$\|D_{ik}\| = 0. \tag{11}$$

This results in a sextic equation for p. Since the eigenvalues p are all non-real [11, 13], there are three pairs of complex conjugates for p which will be denoted by p_L and $\bar{p}_L$ ($L = 1, 2, 3$) where an over bar denotes the complex conjugate, and three pairs of associated eigenvectors $v_{i,L}$ and $\bar{v}_{i,L}$ ($L = 1, 2, 3$). It should be pointed out that some elements of τ_{ij} given by eqn (9) are related to each other. We can show from eqns (4), (8) and (9) that $\tau_{ij} = \tau_{ji}$ and

$$\left.\begin{aligned} \tau_{12} &= -p\tau_{13}, \\ \tau_{22} &= -p\tau_{23} = p^2\tau_{33}. \end{aligned}\right\} \tag{12}$$

They agree with Lekhnitskii's results in [11] except that τ_{33} is taken as unity in [11]. However, τ_{33} may vanish in degenerate cases [12] and hence Lekhnitskii's approach requires a special treatment whenever $\tau_{33} = 0$.

The general solution for the displacements and stresses can now be written as

$$u_i = \sum_L \{v_{i,L} f_L(Z_L) + \bar{v}_{i,L} g_L(\bar{Z}_L)\} \tag{13}$$

$$\sigma_{ij} = \sum_L \{\tau_{ij,L} \mathrm{d}f_L(Z_L)/\mathrm{d}Z_L + \bar{\tau}_{ij,L} \mathrm{d}g_L(\bar{Z}_L)/\mathrm{d}\bar{Z}_L\} \tag{14}$$

where the summation is over $L = 1, 2, 3$ and f_L and g_L are, respectively, arbitrary functions of Z_L and $\bar{Z}_L$. Notice that eqn (13) contains six arbitrary functions. When p has a double root, the solution given by eqn (13) is not general unless one has two independent v_i associated with the double root p. Similarly, eqn (13) may not be a general solution when p is a triple root. A modified solution which maintains its generality when p has a multiple root was given in [20]. For isotropic materials, $p = i$ and is a triple root. However, one of the triple roots is associated with the anti-plane deformation while the other two which can be considered a double root are associated with plane strain deformations[21].

To study the singularities at a crack tip, we let

$$\left.\begin{aligned} f_L(Z_L) &= A_L Z_L^{1-\kappa}/(1-\kappa) \\ g_L(\bar{Z}_L) &= B_L \bar{Z}_L^{1-\kappa}/(1-\kappa) \end{aligned}\right\} \quad (L \text{ not summed}) \tag{15}$$

where κ, A_L and B_L are arbitrary constants which may be complex. Introducing the polar coordinates (r, ϕ):

$$x_2 = r\cos\phi, \; x_3 = r\sin\phi. \tag{16}$$

Equations (13) and (14) can be written as

$$u_i = r^{1-\kappa} \sum_L \{A_L v_{i,L} \zeta_L^{1-\kappa} + B_L \bar{v}_{i,L} \bar{\zeta}_L^{1-\kappa}\}/(1-\kappa) \tag{17}$$

$$\sigma_{ij} = r^{-\kappa} \sum_L \{A_L \tau_{ij,L} \zeta_L^{-\kappa} + B_L \bar{\tau}_{ij,L} \bar{\zeta}_L^{-\kappa}\} \tag{18}$$

where

$$\zeta_L = \cos\phi + p_L \sin\phi. \tag{19}$$

We see that if the real part of κ is positive, σ_{ij} is singular at $r = 0$.

When κ is real, one may choose without loss of generality[1]

$$B_L = \bar{A}_L = (a_L + i\tilde{a}_L)/2 \tag{20}$$

where a_L and $\tilde{a}_L$ are real constants. Equations (17) and (18) then have the real expressions

$$u_i = r^{1-\kappa} \sum_L \{a_L \mathrm{Re}(v_{i,L}\zeta_L^{1-\kappa}) + \tilde{a}_L \mathrm{Im}(v_{i,L}\zeta_L^{1-\kappa})\}/(1-\kappa) \tag{21}$$

$$\sigma_{ij} = r^{-\kappa} \sum_L \{a_L \mathrm{Re}(\tau_{ij,L}\zeta_L^{-\kappa}) + \tilde{a}_L \mathrm{Im}(\tau_{ij,L}\zeta_L^{-\kappa})\} \tag{22}$$

where Re and Im stand for real and imaginary, respectively.

We may also use c_{ij} instead of c_{ijkp} and write eqns (2) and (4) as

$$\sigma_i = c_{ij}\epsilon_j, \quad c_{ij} = c_{ji} \tag{23}$$

where

$$\left.\begin{matrix} \sigma_1 = \sigma_{11}, & \sigma_2 = \sigma_{22}, & \sigma_3 = \sigma_{33} \\ \sigma_4 = \sigma_{23}, & \sigma_5 = \sigma_{13}, & \sigma_6 = \sigma_{12} \end{matrix}\right\} \tag{24a}$$

$$\left.\begin{matrix} \epsilon_1 = \epsilon_{11}, & \epsilon_2 = \epsilon_{22}, & \epsilon_3 = \epsilon_{33} \\ \epsilon_4 = 2\epsilon_{23}, & \epsilon_5 = 2\epsilon_{13}, & \epsilon_6 = 2\epsilon_{12}. \end{matrix}\right\} \tag{24b}$$

We will also write the inverse of eqn (23) as

$$\epsilon_i = s_{ij}\sigma_j, \quad s_{ij} = s_{ji} \tag{25}$$

where s_{ij} are the elastic compliances.

3. SINGULARITIES AT A CRACK TIP IN A HOMOGENEOUS ANISOTROPIC MATERIAL

In this section we assume that material 1 and material 2 in Fig. 2 are the same material. Therefore, there is no interface and the crack is in a homogeneous medium. This problem has been studied in [16, 17] where the material property is assumed to be symmetric with respect to the $x_1 = 0$ plane. No symmetry is assumed in this section. Sih and Chen[18] and Hoenig[19] also studied the problem without assuming the symmetry, but the analysis presented here will show that $\kappa = \frac{1}{2}$ is a root of multiplicity three. The boundary conditions at the crack surface are

$$\sigma_{3j} = 0 \text{ at } \phi = \pm\pi. \tag{26}$$

From eqn (19) we have

$$\zeta_L = \mathrm{e}^{\pm\pi i} \text{ at } \phi = \pm\pi \tag{27}$$

and application of eqn (26) to (18) yields

$$\sum_L \{A_L \tau_{3j,L} \mathrm{e}^{-\kappa\pi i} + B_L \bar{\tau}_{3j,L} \mathrm{e}^{\kappa\pi i}\} = 0 \tag{28}$$

$$\sum_L \{A_L \tau_{3j,L} \mathrm{e}^{\kappa\pi i} + B_L \bar{\tau}_{3j,L} \mathrm{e}^{-\kappa\pi i}\} = 0 \tag{29}$$

where $j = 1, 2, 3$. Equations (28) and (29) may be written in matrix notation as

$$\mathbf{K}(\kappa)\mathbf{q} = \mathbf{0} \tag{30}$$

where $\mathbf{q}$ is a column matrix whose elements are A_L and B_L ($L = 1, 2, 3$), while $\mathbf{K}$ is a 6×6 square matrix and is a function of κ. For a nontrivial solution of $\mathbf{q}$ we must have

$$\|\mathbf{K}(\kappa)\| = 0 \tag{31}$$

which provides the roots κ.

Notice that when $\kappa = \frac{1}{2}$, $e^{\kappa\pi i} = -e^{-\kappa\pi i} = i$ and the l.h.s. of eqn (28) is identical to that of eqn (29) except the minus signs. Hence the first three rows of **K** are identical to the last three rows except the signs and the rank of **K** is no more than 3. This means that $\kappa = \frac{1}{2}$ is a root of multiplicity of at least 3 and that there are at least 3 independent solutions for **q** in eqn (30) associated with $\kappa = \frac{1}{2}$.

To find **q**, i.e. A_L and B_L for $\kappa = \frac{1}{2}$, let

$$\sum_L \tau_{3j,L}\tau^*_{3s,L} = J\delta_{js}, \quad J = \|\tau_{3j,L}\| \tag{32}$$

where δ_{js} is the Kronecker delta. Thus regarding $\tau_{3j,L}$ as a 3×3 matrix, $\tau^*_{3j,L}$ is the adjoint matrix and J is the determinant. Assuming that $J \neq 0$, the solution given by

$$A_L = \frac{1}{2\sqrt{2}} J^{-1} k_s \tau^*_{3s,L}, \; B_L = \frac{1}{2\sqrt{2}} \bar{J}^{-1} k_s \bar{\tau}^*_{3s,L} \tag{33}$$

satisfies eqns (28) and (29) when $\kappa = \frac{1}{2}$. k_s $(s = 1, 2, 3)$ in eqn (33) are arbitrary real constants. With eqn (33), eqn (18) can now be written as, noticing that $\kappa = \frac{1}{2}$,

$$\sigma_{ij}(r, \phi) = \frac{1}{(2r)^{\frac{1}{2}}} \sum_L \mathrm{Re}\left\{J^{-1}\tau^*_{3s,L}\tau_{ij,L}\zeta_L^{-\frac{1}{2}}\right\}k_s. \tag{34}$$

Equation (34) provides three independent solutions for the stress distribution near the crack tip. Notice that at $\phi = 0$, eqn (34) for $i = 3$ has the expression, after using eqn (19) and (32),

$$\sigma_{3j}(r, 0) = \frac{1}{(2r)^{\frac{1}{2}}} k_j, \; j = 1, 2, 3. \tag{35}$$

Hence k_j are the stress intensity factors. It is shown in the Appendix that the solution associated with k_3 can be identified with the solution near the tip of a crack length $2a$ due to a uniform symmetric tensile stress σ_{33} at infinity. Similarly, the solutions associated with k_1 and k_2 can be identified with the solutions near the tip of a crack length $2a$ due to uniform antisymmetric shear stresses σ_{31} and σ_{32}, respectively, at infinity.

Equation (34) is not valid when $J = 0$. However, $J = 0$ implies that $\bar{J} = 0$ and the rank of **K** is no more than two. It follows that $\kappa = \frac{1}{2}$ is a root of multiplicity of at least four when $J = 0$. This is not possible because for the special case of a crack in an isotropic material it is known that $\kappa = \frac{1}{2}$ is a root of multiplicity three.

4. SINGULARITIES AT THE TIP OF A CRACK NORMAL TO AN INTERFACE

We will now proceed to determine the singularities at the tip of a crack which is normal to the interface between two anisotropic materials as shown in Fig. 2. Equations (17) and (18) for the displacements and the stresses apply to materials 1 and 2. To distinguish notations in material 2 from those in material 1, we will add a prime to all notations referring to material 2 except κ which is the same in both materials and r and ϕ which have unambiguous definitions. Since material 1 is divided into two parts by a crack, the displacements and the stresses in both parts need not be given by the same expressions. We will therefore use a superscript $(+)$ to denote quantities referred to material 1 in the $x_3 > 0$ region and a superscipt $(-)$ to denote quantities referred to material 1 in the $x_3 < 0$ region.

The stress-free boundary conditions at the crack surface are

$$\left.\begin{aligned} \sigma^+_{3j} &= 0 \text{ at } \phi = \pi \\ \sigma^-_{3j} &= 0 \text{ at } \phi = -\pi \end{aligned}\right\} \tag{36a}$$

and the continuity conditions at the interface are

$$\left.\begin{aligned} u_i^+ - u_i' &= 0 \\ \sigma_{2j}^+ - \sigma_{2j}' &= 0 \end{aligned}\right\} \text{at } \phi = \pi/2 \tag{36b}$$

$$\left.\begin{aligned} u_i' - u_i^- &= 0 \\ \sigma_{2j}' - \sigma_{2j}^- &= 0 \end{aligned}\right\} \text{at } \phi = -\pi/2 \tag{36c}$$

where $i,j = 1, 2, 3$. Use of the expressions for u_i and σ_{ij} from eqns (17) and (18) in eqn (36a), (36b), (36c) results in 18 equations for the eighteen coefficients A_L^+, B_L^+, A_L', B_L', A_L^- and B_L^- $(L = 1, 2, 3)$ which can again be written in the form

$$\mathbf{K}(\kappa)\mathbf{q} = \mathbf{0} \tag{37}$$

where $\mathbf{K}$ is now an 18×18 square matrix and the elements of $\mathbf{q}$ are A_L^+, B_L^+, A_L', B_L', A_L^- and B_L^- $(L = 1, 2, 3)$. For a nontrivial solution of $\mathbf{q}$, we must have

$$\|\mathbf{K}(\kappa)\| = 0. \tag{38}$$

It should be pointed out that for real κ one could use the real expressions for u_i and σ_{ij} in eqns (21) and (22). We again obtain 18 equations in the form of eqn (37) in which the elements of $\mathbf{q}$ are a_L^+, $\tilde{a}_L^+$, a_L', $\tilde{a}_L'$, a_i^- and $\tilde{a}_L^-$. The elements of the 18×18 matrix $\mathbf{K}$ are real.

The roots κ of eqn (38), whether real or complex, can be found numerically when the elasticity constants c_{ij} and c_{ij}' of both materials are known. In the complex plane κ, one can find the number of roots κ in a given region by using the following theorem[22]: If a function $\psi(\kappa)$, whose only singularities inside a closed contour C of the κ-plane are poles and whose value is not zero at any point on the contour, then

$$\frac{1}{2\pi i}\int_C \frac{d\psi/d\kappa}{\psi}\, d\kappa = N - P \tag{39}$$

where N is the number of zeros and P is the number of poles inside C. In our problem $\psi = \|\mathbf{K}\|$ and eqn (39) can be written as

$$\frac{1}{2\pi i}\int_C d\{\ln \|K\|\} = N \tag{40}$$

because $\|\mathbf{K}\|$ is bounded and hence there is no pole. In view of the fact that

$$\ln \psi = \ln |\psi| + i \arg \psi. \tag{41}$$

Equation (40) reduces to

$$N = \frac{1}{2\pi}(\arg \|\mathbf{K}\|)_C \tag{42}$$

where $(f)_C$ denotes the change in the value of f in going around the contour C. Equation (42) implies that *if $\|K\|$ has N roots inside the contour C in the κ-plane, the locus of $\|K\|$ when plotted on the complex $\|K\|$ plane encircles the origin N times as κ goes around the contour C.* This is a useful result which can be employed to determine the number of roots in a given region.

5. NUMERICAL EXAMPLES

For numerical examples we will assume that each layer in the composite shown in Fig. 1 is an orthotropic material with respect to the $(\hat{x}_1, \hat{x}_2, \hat{x}_3)$ axes where $\hat{x}_2 = x_2$ and the $\hat{x}_3$-axis is the fiber direction which makes an angle θ with the x_3-axis. We further assume that all layers are identical orthotropic materials although the ply-angle θ may vary from layer to layer. Referring to the $(\hat{x}_1, \hat{x}_2, \hat{x}_3)$ axes, the following engineering constants for two different orthotropic materials are taken from [23, 24], respectively.

Composite W

(Typical high modulus graphite/epoxy, [23])

$$\left.\begin{aligned} &E_1 = E_2 = 2.1 \times 10^6 \text{ psi} \\ &E_3 = 20 \times 10^6 \text{ psi} \\ &G_{12} = G_{23} = G_{31} = 0.85 \times 10^6 \text{ psi} \\ &\nu_{21} = \nu_{31} = \nu_{32} = 0.21 \end{aligned}\right\} \tag{43}$$

Composite T

(T300/5208 graphite/epoxy, [24])

$$\left.\begin{aligned} &E_1 = E_2 = 1.54 \times 10^6 \text{ psi} \\ &E_3 = (20 \times 10^6 \text{ psi})\dagger \\ &G_{12} = G_{23} = G_{31} = 0.81 \times 10^6 \text{ psi} \\ &\nu_{21} = \nu_{31} = \nu_{32} = 0.28. \end{aligned}\right\} \tag{44}$$

In eqns (43) and (44), E_i are the Young's moduli, G_{ij} the shear moduli and ν_{ij} are the Poisson's ratios[25]. They are related to s_{ij}[25, 26], and hence s_{ij} can be computed. Since E_{ij}, G_{ij} and ν_{ij} given in eqns (43) and (44) are referred to the $(\hat{x}_1, \hat{x}_2, \hat{x}_3)$ axes, s_{ij} so obtained will be denoted by $\hat{s}_{ij}$. Its inverse $\hat{c}_{ij}$ is obtained by using the equations derived in [25]. Finally, we obtain s_{ij} and c_{ij} which are referred to the (x_1, x_2, x_3) axes from $\hat{s}_{ij}$ and $\hat{c}_{ij}$ (see [2, 12]) when the ply-angle θ in material 1 is given. For a different ply-angle θ' in material 2, we obtain s'_{ij} and c'_{ij} in the same way.

With the elasticity constants c_{ij} and c'_{ij} associated with the ply-angles θ and θ' in materials 1 and 2 so determined, the formulation in Section 4 provides the matrix $\mathbf{K}$ and the roots of the determinant $\|\mathbf{K}\|$ furnish the desired roots. In Table 1 we list the roots κ for the Composite W given by eqn (43) for combinations of (θ/θ') angles in which both θ and θ' assume the values between $-90°$ and $90°$ with an increment of 15°. Since the values of κ for $(-a/b)$ and $(a/-b)$ composites are identical, it is sufficient to consider $\theta > 0$ only. In Table 2 we list the roots κ for composite T. In both tables, $\kappa = \frac{1}{2}$ is a triple root when $\theta = \theta'$ and when $\theta = -\theta' = 90°$. This is expected since when $\theta = \theta'$ and $\theta = -\theta' = 90°$ material 1 and material 2 have the same fiber oritentation and hence there is no real interface between material 1 and material 2. Thus the crack is in a homogeneous material and the analysis in Section 3 shows that $\kappa = \frac{1}{2}$ is a triple root. For all other combinations of (θ/θ') there are three non-equal roots of positive κ.

Notice that the values of κ are identical for $(\theta/90)$ and $(\theta/-90)$. Likewise, κ's are identical for $(0/\theta')$ and $(0/-\theta')$ as well as for $(90/\theta')$ and $(90/-\theta')$. Some of the roots are not easy to locate. For instance, two of the three roots for (0/90) in Composite T differ by only 10^{-5}. At the first calculation we only located the root $\kappa = 0.697726$ and completely missed the other two roots. Great effort and care were exercised in locating the two roots which are very close to each other. We also used eqn (42) to verify numerically that there are indeed three positive roots for κ.

†The value of E_3 in [24] is 22×10^6 psi. The calculations presented in Table 2 and Figs. 4 and 6 were inadvertently based on $E_3 = 20 \times 10^6$ psi. However, a few sample calculations with the correct E_3 show that the errors on κ are no more than 1%.

Table 1. Values of κ for the $r^{-\kappa}$ singularity in Composite W

θ' \ θ	0	15°	30°	45°	60°	75°	90°
90°	.676635 .500212 .5	.676012 .502156 .500222	.672441 .505068 .500236	.660488 .504813 .500227	.630471 .502297 .500165	.567537 .500314 .500048	.5
75°	.675051 .500189 .433918	.665411 .500305 .446234	.646234 .500401 .466560	.616354 .500415 .485037	.571159 .500269 .496300	.5	.499859 .499688 .432561
60°	.665263 .499839 .379767	.642118 .500352 .404849	.605628 .500735 .441810	.557636 .500673 .477316	.5	.503704 .499085 .430024	.498608 .497668 .371402
45°	.643963 .499012 .369508	.606474 .500092 .407075	.556388 .500639 .456342	.5	.522801 .498293 .443947	.515052 .496531 .388842	.495691 .495008 .345965
30°	.609394 .498562 .391694	.557954 .499986 .442491	.5	.543655 .498192 .445399	.558434 .495380 .400299	.533668 .493226 .364378	.494600 .492252 .339747
15°	.560499 .499279 .438704	.5	.557552 .498554 .444039	.592813 .495627 .400073	.595139 .492603 .369244	.553905 .490548 .349787	.497659 .489828 .340358
0	.5	.562178 .498904 .441309	.609785 .496201 .397243	.631434 .493110 .367864	.620457 .490626 .350305	.566078 .489298 .342401	.5 .489038 .341108
-15°	.560499 .499279 .438704	.612345 .497112 .392438	.644542 .494473 .364451	.651651 .492080 .349195	.628243 .490464 .342609	.564345 .489824 .341721	.497659 .489828 .340358
-30°	.609394 .498562 .391684	.645821 .496706 .361115	.662510 .494839 .347946	.656327 .493276 .344694	.621931 .492378 .346998	.552727 .492163 .349080	.494600 .492252 .339747
-45°	.643963 .499012 .369508	.665377 .497882 .352528	.668725 .496774 .351288	.651255 .495887 .357999	.608061 .495504 .367486	.538511 .495550 .368791	.495691 .495008 .345965
-60°	.665263 .499839 .379767	.674013 .499331 .373635	.666989 .498824 .381746	.641375 .498455 .396175	.592892 .498378 .410685	.526260 .498488 .409137	.498608 .497668 .371402
-75°	.675051 .500189 .433918	.674923 .500080 .435943	.663730 .499972 .447918	.638493 .499903 .462126	.593334 .499878 .474130	.523618 .499848 .476682	.499859 .499688 .432561
-90°	.676635 .500212 .5	.676012 .502156 .500222	.672441 .505068 .500236	.660488 .504813 .500227	.630471 .502297 .500165	.567537 .500314 .500048	.5

The results presented in Table 1 and 2 are shown in graphs in Figs. 3–6. In Fig. 3 contour lines for the largest κ, denoted by κ_1, are shown for Composite W and the corresponding contour lines for Composite T is shown in Fig. 4. In Figs. 5 and 6 the contour lines for $(\kappa_1 - \kappa_3)$ where κ_3 is the smallest of the three roots are shown for Composite W and Composite T, respectively. In view of symmetry, only half of the contour lines are shown in Figs. 3–6. In both composites we see that the largest κ_1 occurs at $(0/-90)$ which is identical to $(0/90)$. At $(0/90)$, $\kappa_1 = 0.676635$ for Composite W and $\kappa_1 = 0.697726$ for Composite T. The largest difference between κ_1 and κ_3 occurs approximately at $(30/-40)$ for both Composite W and Composite T.

6. UNIFORM EXTENSION

We will consider in this section the problem in which the composite shown in Fig. 2 is subject to a uniform extensional strain ϵ_1 in the x_1-direction. For this purpose, we add the term $\epsilon_1 \delta_{i1} x_1$ to the r.h.s. of eqns (5), (13), (17) and (21) for the displacements u_i and

Table 2. Values of κ for the $r^{-\kappa}$ singularity in Composite T

θ' \ θ	0	15°	30°	45°	60°	75°	90°
90°	.697726 .5 .499990	.695390 .501422 .499970	.687400 .503731 .499959	.670249 .504020 .500004	.636110 .502055 .500055	.570493 .500028 .499923	.5
75°	.694552 .499899 .433166	.682182 .499923 .446108	.658683 .500018 .465858	.623468 .500173 .484789	.573597 .500205 .496796	.5	.500075 .499786 .429903
60°	.681455 .499252 .380013	.655864 .499572 .405261	.615433 .500057 .440977	.562256 .500366 .476460	.5	.503193 .499057 .428481	.498302 .497881 .367957
45°	.655675 .498169 .370945	.615621 .499132 .408413	.561314 .500048 .456362	.5	.523662 .498551 .440550	.515275 .496552 .385476	.496507 .496224 .341936
30°	.615974 .497892 .393350	.561933 .499414 .443807	.5	.543669 .498709 .441797	.559222 .496016 .394947	.534343 .493379 .359462	.495858 .491924 .334337
15°	.562542 .499066 .439371	.5	.556290 .499047 .441155	.591495 .496372 .395197	.594666 .493174 .363520	.553999 .490735 .343852	.498878 .489680 .333397
0	.5	.561734 .499106 .439862	.608589 .496752 .393682	.630402 .493751 .362960	.620348 .491033 .344491	.566821 .489363 .335554	.5 .488944 .333540
-15°	.562542 .499066 .439371	.614806 .497105 .391399	.646999 .494775 .361050	.654617 .492462 .344079	.632281 .490645 .335970	.568975 .489711 .333613	.498878 .489680 .333397
-30°	.615974 .497892 .393350	.653467 .496339 .360418	.670723 .494834 .344095	.665388 .493407 .338249	.632110 .492360 .338301	.562294 .491864 .339280	.495858 .491924 .334337
-45°	.655675 .498169 .370945	.678402 .497416 .350987	.682644 .496660 .345625	.666150 .495899 .348752	.623644 .495381 .355521	.551195 .495156 .357113	.496507 .496244 .341936
-60°	.681455 .499252 .380013	.691616 .499019 .370260	.685470 .498713 .373343	.660390 .498389 .383591	.611548 .498218 .395570	.539832 .498183 .396061	.498302 .497881 .367957
-75°	.694552 .499899 .433166	.695563 .499852 .431371	.684047 .499759 .438689	.657219 .499696 .450101	.609624 .499704 .461274	.537075 .499720 .463714	.500075 .499786 .429903
-90°	.697726 .5 .499990	.695390 .501422 .499970	.687400 .503731 .499959	.670249 .504020 .500004	.636110 .502055 .500055	.570493 .500028 .499923	.5

the term $c_{ij11}\epsilon_1$ to eqns (7), (14), (18) and (22) for the stresses σ_{ij}[1, 27]. With these modifications, application of the boundary and interface conditions, eqns (36), results in the following system of equations

$$r^{-\kappa}\mathbf{K}(\kappa)\mathbf{q} = \epsilon_1\mathbf{b} \tag{45}$$

where the elements of $\mathbf{q}$ are A_L^+, B_L^+, A_L', B_L', A_L^- and B_L^- while $\mathbf{b}$ contains c_{ij11}. Since the r.h.s. of eqn (45) is independent of r, we let $\kappa = 0$ and obtain

$$\mathbf{K}(0)\mathbf{q} = \epsilon_1\mathbf{b}. \tag{46}$$

Equation (46) provides $\mathbf{q}$ if $\mathbf{K}(0)$ is not singular. If $\mathbf{K}(0)$ is singular, a solution may still exist if $\mathbf{b}$ is orthogonal to the left eigenvectors of $\mathbf{K}(0)$. However, when $\kappa = 0$ eqn (18) indicates that σ_{ij} are constants and the stresses are uniform. Therefore, instead of solving

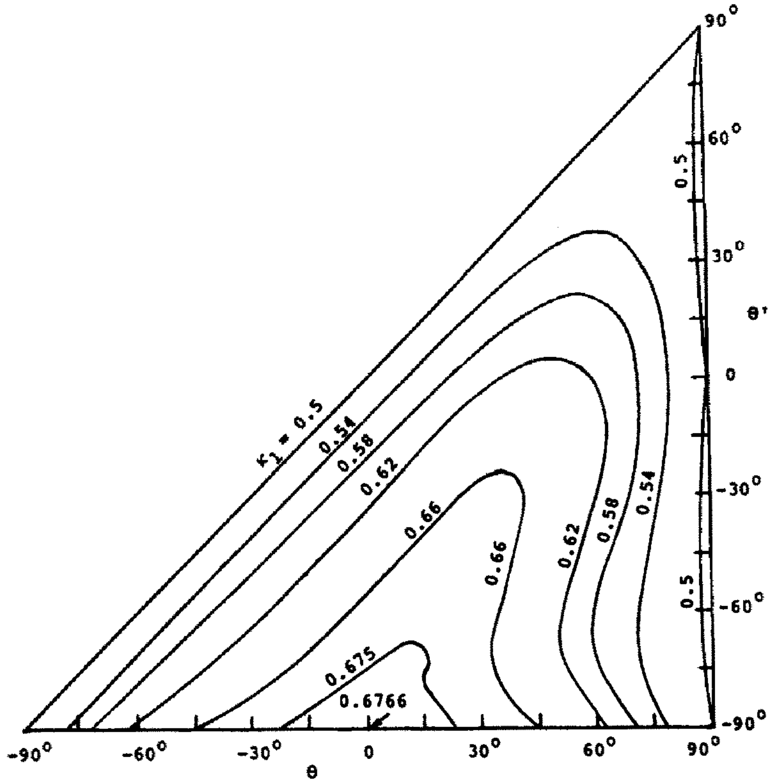

Fig. 3. Contour lines for κ_1, the largest κ of the $r^{-\kappa}$ singularity for Composite W.

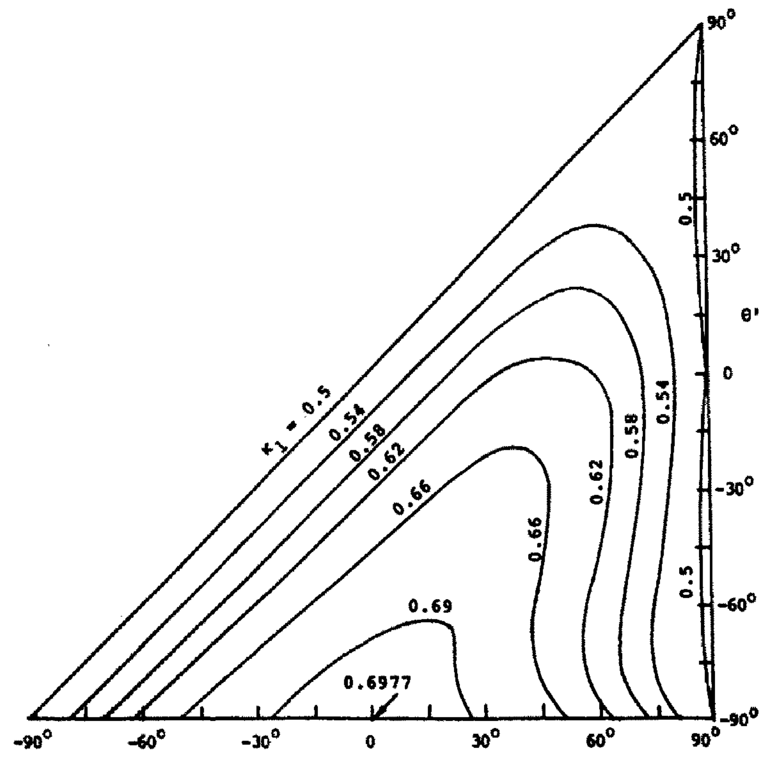

Fig. 4. Contour lines for κ_1, the largest κ of the $r^{-\kappa}$ singularity for Composite T.

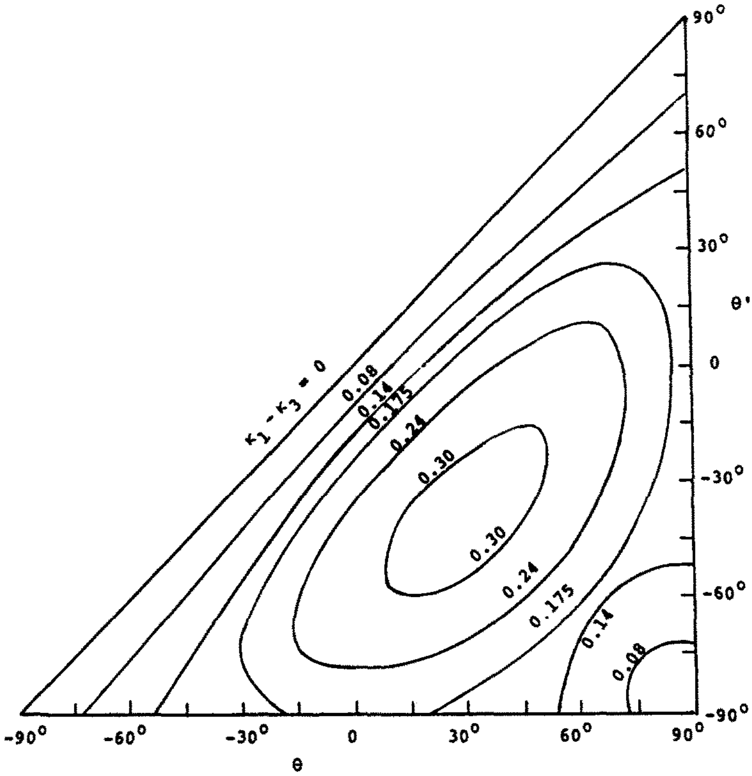

Fig. 5. Contour lines for the difference between the largest (κ_1) and the smallest (κ_3) singularites for Composite *W*.

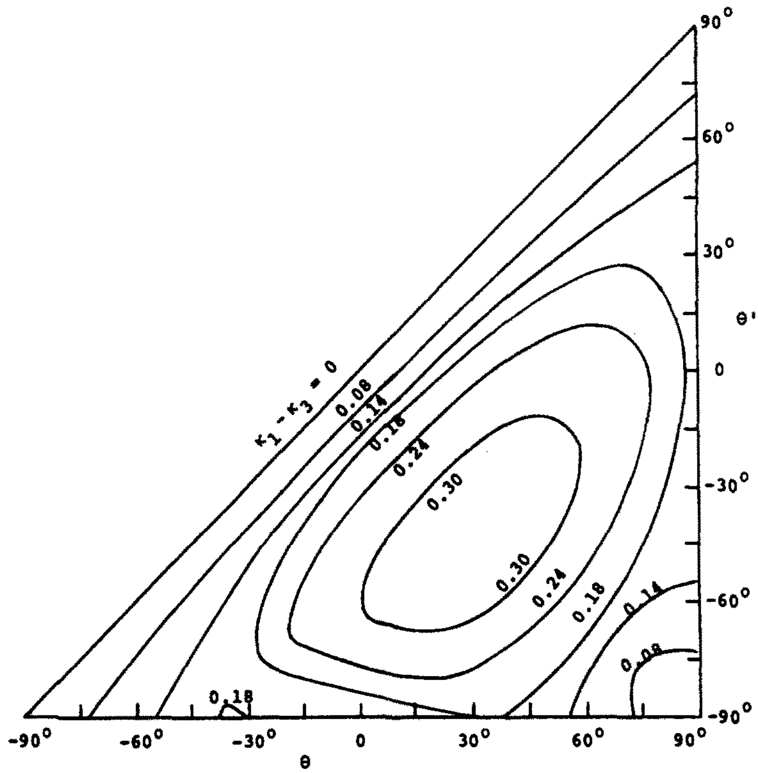

Fig. 6. Contour lines for the difference between the largest (κ_1) and the smallest (κ_3) singularities for Composite *T*.

eqn (46), we will use an alternate approach employed in [1] to find a uniform stress solution which satisfies the prescribed uniform extensional strain ϵ_1.

To this end, we first solve σ_1 from the first of eqn (25):

$$\sigma_1 = (\epsilon_1/s_{11}) - R_j\sigma_j, \quad (j \neq 1). \tag{47}$$

We then eliminate σ_1 from the rest of eqn (25) to obtain

$$\epsilon_i = R_{ij}\sigma_j + R_i\epsilon_1, \quad (i \neq 1, j \neq 1) \tag{48}$$

where

$$\left.\begin{aligned} R_i &= s_{i1}/s_{11} \\ R_{ij} &= s_{ij} - s_{i1}R_j \end{aligned}\right\} \tag{49}$$

The free surface conditions, eqn (36a), imply that

$$\left.\begin{aligned} \sigma_3^+ &= \sigma_4^+ = \sigma_5^+ = 0 \\ \sigma_3^- &= \sigma_4^- = \sigma_5^- = 0 \end{aligned}\right\} \tag{50}$$

in the entire region occupied by material 1 because the stresses are uniform. The continuity conditions across the interface $\phi = \pm\pi/2$ as given by eqns (36b, c) can be shown to be equivalent to

$$\left.\begin{aligned} \epsilon_1^+ &= \epsilon_1' = \epsilon_1^- \quad \epsilon_3^+ = \epsilon_3' = \epsilon_3^- \quad \epsilon_5^+ = \epsilon_5' = \epsilon_5^- \\ \sigma_2^+ &= \sigma_2' = \sigma_2^- \quad \sigma_4^+ = \sigma_4' = \sigma_4^- \quad \sigma_6^+ = \sigma_6' = \sigma_6^- . \end{aligned}\right\} \tag{51}$$

From eqns (50) and (51), the stresses σ_i^+, σ_i^- and σ_i' in the regions $\pi/2 < \phi < \pi$, $-\pi < \phi < -\pi/2$ and $-\pi/2 < \phi < \pi/2$, respectively, have the following non-zero components:

$$\left.\begin{aligned} \sigma_i^+ &= (\sigma_1^+, \sigma_2, 0, 0, 0, \sigma_6) \\ \sigma_i^- &= (\sigma_1^-, \sigma_2, 0, 0, 0, \sigma_6) \\ \sigma_i' &= (\sigma_1', \sigma_2, \sigma_3', 0, \sigma_5', \sigma_6) \end{aligned}\right\} \tag{52}$$

where the superscripts $+$, $-$ and a prime are omitted for σ_2 and σ_6 in view of eqn (51). Using eqn (52) in eqn (48), the expressions ϵ_3 and ϵ_5 in material 1 are

$$\left.\begin{aligned} \epsilon_3 &= R_{32}\sigma_2 + R_{36}\sigma_6 + R_3\epsilon_1 \\ \epsilon_5 &= R_{52}\sigma_2 + R_{56}\sigma_6 + R_5\epsilon_1 \end{aligned}\right\} \tag{53}$$

while the expressions for ϵ_3 and ϵ_5 in material 2 are

$$\left.\begin{aligned} \epsilon_3 &= R_{32}'\sigma_2 + R_{33}'\sigma_3' + R_{35}'\sigma_5' + R_{36}'\sigma_6 + R_3'\epsilon_1 \\ \epsilon_5 &= R_{52}'\sigma_2 + R_{53}'\sigma_3' + R_{55}'\sigma_5' + R_{56}'\sigma_6 + R_5'\epsilon_1 . \end{aligned}\right\} \tag{54}$$

Again, the superscripts $+$, $-$ and a prime for ϵ_3 and ϵ_5 are omitted in view of eqn (51).

For the composite considered in eqn (43) and (44), the material property in each layer is symmetric with respect to the $x_2 = 0$ plane and hence[24, 25],

$$s_{14} = s_{16} = s_{24} = s_{26} = s_{34} = s_{36} = s_{54} = s_{56} = 0. \tag{55}$$

This implies that $R_{36} = R_{36}' = R_{56} = R_{56}' = 0$ and elimination of ϵ_3 and ϵ_5 from eqns (53) and (54) reduces to

$$\left.\begin{aligned} (R_{32}' - R_{32})\sigma_2 + R_{33}'\sigma_3' + R_{35}'\sigma_5' &= -(R_3' - R_3)\epsilon_1 \\ (R_{52}' - R_{52})\sigma_2 + R_{53}'\sigma_3' + R_{55}'\sigma_5' &= -(R_5' - R_5)\epsilon_1 . \end{aligned}\right\} \tag{56}$$

Equations (56) provide a one-parameter family of solutions for σ_2, σ_3' and σ_5'. σ_6 is arbitrary while σ_1^+, σ_1^- and σ_1' are determined from eqn (47). This completes the solution for non-zero elements of the stresses shown in eqn (52). It is not difficult to see from eqns (52) and (47) that $\sigma_1^+ = \sigma_1^-$.

Equations (56) have no solutions if

$$\frac{R_{32}' - R_{32}}{R_{52}' - R_{52}} = \frac{R_{33}'}{R_{53}'} = \frac{R_{35}'}{R_{55}'} \neq \frac{R_3' - R_3}{R_5' - R_5}. \tag{57}$$

For the composites considered here, eqns (57) do not hold and a uniform stress solution exists for a given extensional strain ϵ_1. Hence, there is no additional stress singularity at the crack tip due to the uniform extension for the composites considered here. If eqns (57) held, one would have a logarithmic stress singularity at the crack tip [1].

7. CONCLUDING REMARKS

We have shown that the stress singularity at the tip of a crack which is normal to and ends at an interface between two anisotropic elastic media has the form $r^{-\kappa}$ where κ is a root of eqn (38). We show that there are in general three distinct positive roots of κ, say κ_s ($s = 1, 2, 3$). For each κ_s, eqn (37) furnishes the associated $\mathbf{q}_s$ whose elements are A_L, B_L in eqn (18). Since $\mathbf{q}_s$ is unique up to a multiplicative constant, say c_s, the solution given by eqn (18) for $\kappa = \kappa_1$, κ_2 and κ_3 can be superimposed and written as

$$\sigma_{ij} = c_1 r^{-\kappa_1} \sigma_{ij}^{(1)} + c_2 r^{-\kappa_2} \sigma_{ij}^{(2)} + c_3 r^{-\kappa_3} \sigma_{ij}^{(3)} \tag{58}$$

where $\sigma_{ij}^{(s)}$ ($s = 1, 2, 3$) are known functions of ϕ. The analysis presented here provides κ_s and $\sigma_{ij}^{(s)}$ ($s = 1, 2, 3$). The unknown constants c_1, c_2 and c_3 have to be determined from the complete boundary conditions of the whole composite. One could use the solution obtained here to form a special finite element at the crack tip and use regular finite elements elsewhere to find a complete solution numerically for the stress distribution in the composite with a crack.

It should be pointed out that eqn (38) provides, besides the three positive κ presented here, infinitely many κ whose real part is negative. Thus to increase the accuracy in the special finite element at the crack tip, one may add as many terms as one pleases to the r.h.s. of eqn (58). These additional terms are non-singular at the tip of the crack.

Acknowledgements—The work presented here is supported by the Army Materials and Mechanics Research Center, Watertown, Massachusetts, through contract DAAG 46-81-K-0086. Special thanks are due to Dr. S. C. Chou, the technical monitor, for valuable discussions during the course of this study. We also thank Mr. Dong K. Nguyen for his assistant in some of the computer calculations.

REFERENCES

1. R. I. Zwiers, T. C. T. Ting and R. L. Spilker, On the logarithmic singularity of free-edge stress in laminated composites under uniform extension. *J. Appl. Mech.* **49**, 561–569 (1982).
2. R. I. Zwiers and T. C. T. Ting, Free-edge and contact-edge singularities in laminated composites. AMMRC TR 82-21, Dept. of Materials Engineering, Univ. of Illinois at Chicago Circle (April 1982).
3. A. K. Zak and M. L. Williams, Crack point stress singularities at a bi-material interface. *J. Appl. Mech.* **30**, 142–143 (1963).
4. D. B. Bogy, On the plane elastostatic problem of a loaded crack terminating at a material interface. *J. Appl. Mech.* **38**, 911–918 (1971).
5. T. S. Cook and F. Erdogan, Stresses in bonded materials with a crack perpendicular to the interface. *Int. J. Engng Sci.* **10**, 677–697 (1972).
6. G. D. Gupta, A layered composite with a broken laminate. *Int. J. Solids Structures* **9**, 1141–1154 (1973).
7. F. Erdogan and M. Bakioglu, Fracture of plates which consists of periodic dissimilar strips. *Int. J. Fracture* **12**, 71–84 (1976).
8. K. Y. Lin and J. W. Mar, Finite element analysis of stress intensity factors for cracks at a bi-material interface. *Int. J. Fracture* **12**, 521–531 (1976).
9. K. Arin, A note on the fracture of laminated composites. *Lett. Appl. Engng Sci.* **3**, 81–85 (1975).
10. F. Delale and F. Erdogan, Bonded orthotropic strips with cracks. *Int. J. Fracture* **15**, 343–364 (1979).
11. S. G. Lekhnitskii, *Theory of Elasticity on an Anisotropic Elastic Body* (translated by P. Fern). Holden Day, San Francisco (1963).

12. T. C. T. Ting and S. C. Chou, Stress singularities in laminated composites. In *Fracture of Composite Materials* (Edited by G. C. Sih and V. P. Tamuzs), pp. 265–277. Nijhoff, Amsterdam (1982).
13. A. N. Stroh, Steady state problems in anisotropic elasticity. *J. Math. Phys.* **41**, 77–103 (1962).
14. D. M. Barnett and J. Lothe, Line force loadings on anisotropic half-space and wedges. *Phys. Norv.* **8**, 13–22 (1975).
15. P. Chadwick and G. D. Smith, Foundations of the theory of surface waves in anisotropic elastic materials. *Adv. Appl. Mech* **17**, 303–376 (1977).
16. G. C. Sih, P. C. Paris and G. R. Irwin, On cracks in rectilinear anisotropic bodies. *Int. J. Fracture Mech.* **1**, 189–302 (1965).
17. G. C. Sih and H. Liebowitz, Mathematical theories of brittle fracture. *Fracture* (Edited by H. Liebowitz), Vol. II, pp. 115–126. Academic Press, New York (1968).
18. G. C. Sih and E. P. Chen, *Cracks in Composite Materials*, pp. 87–97. Nijhoff, Amsterdam (1981).
19. A. Hoenig, Near-tip behavior of a crack in a plane anisotropic elastic body. *Engng Fracture Mech.* **16**, 393–403 (1982).
20. T. C. T. Ting, Effects of change of reference coordinates on the stress analyses of anisotropic elastic materials. *Int. J. Solids Structures* **18**, 139–152 (1982).
21. T. C. T. Ting and S. C. Chou, Edge singularities in anisotropic composites. *Int. J. Solids Structures* **17**, 1057–1068 (1981).
22. E. G. Phillips, *Functions of a Complex Variable*, pp. 107–108. Oliver and Boyd, New York (1961).
23. A. S. D. Wang and F. W. Crossman, Some new results on edge effects in symmetric composite laminates. *J. Composite Materials* **11**, 92–106 (1977).
24. S. C. Chou, Delamination of T300/5208 Graphite/Epoxy Laminates. In *Fracture of Composite Materials* (Edited by G. C. Sih and V. P. Tamuzs), pp. 247–263. Nijhoff, Amsterdam (1982).
25. R. M. Jones, *Mechanics of Composite Materials*. McGraw-Hill, New York (1975).
26. R. M. Christensen, *Mechanics of Composite Materials*, Wiley-Interscience, New York (1979).
27. R. I. Zwiers and T. C. T. Ting, Singularity of Contact-edge stress in laminated composites under uniform extension. *J. Composite Materials* **17**, 49–63 (1983).

APPENDIX

Consider a crack of length 2a located on the x_2-axis between $x_2 = -a$ and $x_2 = a$ in an infinite anisotropic elastic material subjected to a uniform tensile stress σ_{33}^{∞} as well as a uniform plane shear stress σ_{32}^{∞} (Fig. 7) and a uniform antiplane shear stress σ_{31}^{∞} (not shown in Fig. 7) at infinity. The surface of the crack is stress-free. This problem was studied in [16, 17] in which the material property is assumed to be symmetric with respect to the $x_1 = 0$ plane and in [18, 19] for general anisotropic materials. We will present an alternate expression for the solution in the entire plane, not just near the crack tip as in [19]. For the present problem, it sufficies to consider the associated problem in which the crack surface is subjected to the stresses

$$\sigma_{3j} = -\sigma_{3j}^{\infty} \text{ on } -a < x_2 < a \tag{A1}$$

and the stresses vanish at infinity. To this end, we choose in eqns (13, 14)

$$f_L = \bar{g}_L = A_L\{(Z_L^2 - a^2)^{\frac{1}{2}} - Z_L\}/2 \tag{A2}$$

where A_L are arbitrary complex constants. We then have the solution for the displacements

$$u_i = \sum_L \mathrm{Re}\,\{A_L v_{i,L}((Z_L^2 - a^2)^{\frac{1}{2}} - Z_L)\} \tag{A3}$$

and the stresses

$$\sigma_{ij} = \sum_L \mathrm{Re}\left\{A_L \tau_{ij,L}\left(\frac{Z_L}{(Z_L^2 - a^2)^{\frac{1}{2}}} - 1\right)\right\} \tag{A4}$$

which vanish at infinity. To determine A_L, we apply the boundary conditions, eqn (A1):

$$-\sigma_{3j}^{\infty} = \sum_L \mathrm{Re}\left\{A_L \tau_{3j,L}\left(\frac{x_2}{\pm i(a^2 - x_2^2)^{\frac{1}{2}}} - 1\right)\right\}, \quad -a < x_2 < a. \tag{A5}$$

Equation (A5) is satisfied if we let

$$\sum_L \tau_{3j,L} A_L = \sigma_{3j}^{\infty} \tag{A6}$$

or

$$A_L = J^{-1}\sigma_{3s}^{\infty}\tau_{3s,L}^{*} \tag{A7}$$

where J and $\tau_{3s,L}^{*}$ are defined in eqn (32). We therefore obtain the solution

$$u_i = \sum_L \mathrm{Re}\left\{J^{-1}\tau_{3s,L}^{*} v_{i,L}((Z_L^2 - a^2)^{\frac{1}{2}} - Z_L)\right\}\sigma_{3s}^{\infty} \tag{A8}$$

$$\sigma_{ij} = \sum_L \mathrm{Re}\left\{J^{-1}\tau_{3s,L}^{*}\tau_{ij,L}\left(\frac{Z_L}{(Z_L^2 - a^2)^{\frac{1}{2}}} - 1\right)\right\}\sigma_{3s}^{\infty}. \tag{A9}$$

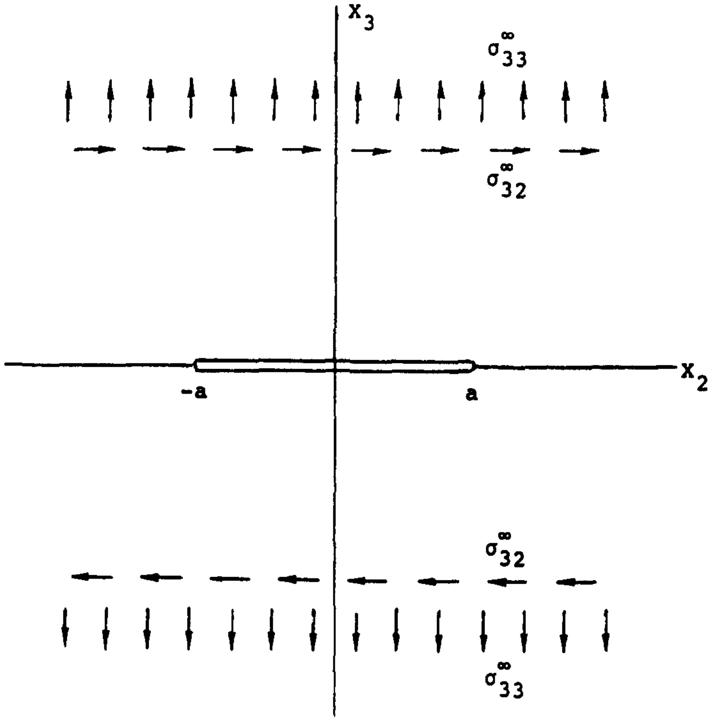

Fig. 7. A crack of length $2a$ subject to uniform stresses at infinity.

To find the stress distribution near the crack tip, say $x_2 = a$, notice that as $Z_L - a \doteq 0$

$$\frac{Z_L}{(Z_L^2 - a^2)^{\frac{1}{2}}} - 1 = \frac{(Z_L - a) + a}{(Z_L - a)^{\frac{1}{2}}(Z_L + a)^{\frac{1}{2}}} - 1 \doteq \left(\frac{a}{2}\right)^{\frac{1}{2}} (Z_L - a)^{-\frac{1}{2}}. \tag{A10}$$

If we let $Z_L - a = r\zeta_L$ and

$$k_s = \sqrt{a}\,\sigma_{3s}^{\infty}, \tag{A11}$$

eqn (A9) reduces to eqn (34). Thus the solution associated with k_3 in eqn (34) is due to the uniform symmetric tensile stress σ_{33}^{∞} applied at infinity while that associated with k_1 and k_2 are due to, respectively, the uniform anti-symmetric shear stresses σ_{31}^{∞} and σ_{32}^{∞} applied at infinity. It should be pointed out that the solution associated with σ_{33}^{∞} is not necessarily symmetric with respect to the x_2 axis even though the loading at the infinity is. Likewise, the solutions associated with σ_{31}^{∞} and σ_{32}^{∞} are not necessarily anti-symmetric with respect to the x_2 axis.